Journal of Archaeological Science: Reports 44 (2022) 103511

Contents lists available at ScienceDirect

Journal of Archaeological Science: Reports

journal homepage: www.elsevier.com/locate/jasrep

High-accuracy methodology for the integrative restoration of archaeological teeth by using reverse engineering techniques and rapid prototyping

Antonino Vazzana [a,*], Owen Alexander Higgins [a], Gregorio Oxilia [a], Federico Lugli [a,c], Sara Silvestrini [a], Alessia Nava [d], Luca Bondioli [a,e,f], Eugenio Bortolini [a,b], Giovanni Di Domenico [g], Federico Bernardini [h,i], Claudio Tuniz [i,j], Lucia Mancini [k,l], Matteo Bettuzzi [m], Maria Pia Morigi [m], Marcello Piperno [n], Carmine Collina [n], Matteo Romandini [a,o], Stefano Benazzi [a,p]

[a] Department of Cultural Heritage, University of Bologna, Ravenna, Italy
[b] Human Ecology and Archaeology (HUMANE), IMF, CSIC, C/Egipciaques 15, 08001 Barcelona, Spain
[c] Department of Chemical and Geological Sciences, University of Modena and Reggio Emilia, Modena, Italy
[d] Human Osteology Lab, School of Anthropology and Conservation, University of Kent, Canterbury, UK
[e] Department of Cultural Heritage, University of Padua, Padua, Italy
[f] Service of Bioarchaeology, Museum of Civilizations, Roma, Italy
[g] Departement of Physics and Earth Sciences, University of Ferrara, Ferrara, Italy
[h] Department of Humanities, Università Ca' Foscari Venezia, Italy
[i] Multidisciplinary Laboratory, Abdus Salam International Centre for Theoretical Physics, Trieste, Italy
[j] Centre for Archaeological Science, University of Wollongong, Northfields Avenue, Wollongong, NSW 2522, Australia
[k] Elettra - Sincrotrone Trieste S.C.p.A., Basovizza, Trieste, Italy
[l] Slovenian National Building and Civil Engineering Institute, Ljubljana, Slovenia
[m] University of Bologna, Department of Physics and Astronomy, Italy
[n] Museo Civico Archeologico Biagio Greco, Mondragone, Italy
[o] Director of the Pradis Cave Museum, Clauzetto, Italy
[p] Department of Human Evolution, Max Planck Institute for Evolutionary Anthropology, Leipzig, Germany

ARTICLE INFO

Keywords:
Tooth reconstruction
Teeth sampling
Digital restoration
Rapid prototyping
Computer-aided design
Reverse engineering

ABSTRACT

The reconstruction of the original morphology of bones and teeth after sampling for physicochemical (e.g., radiocarbon and uranium series dating, stable isotope analysis, paleohistology, trace element analysis) and biomolecular analyses (e.g., ancient DNA, paleoproteomics) is appropriate in many contexts and compulsory when dealing with fossil human remains. The reconstruction protocols available to date are mostly based on manual re-integration of removed portions and can lead to an imprecise recovery of the original morphology.

In this work, to restore the original external morphology of sampled teeth we used computed microtomography (microCT), reverse engineering (RE), computer-aided design (CAD) and rapid prototyping (RP) techniques to fabricate customized missing parts. The protocol was tested by performing the reconstruction of two Upper Palaeolithic human teeth from the archaeological excavations of Roccia San Sebastiano (Mondragone, Caserta, southern Italy) and Riparo I of Grotte Verdi di Pradis (Clauzetto, Pordenone, north-eastern Italy) (RSS2 and Pradis 1, respectively), which were sampled for physicochemical and biomolecular analyses.

It involved a composite procedure consisting in: a) the microCT scanning of the original specimens; b) sampling; c) the microCT scanning of the specimens after sampling; d) the reconstruction of the digital 3D surfaces of the specimens before and after sampling; e) the creation of digital models of the missing/sampled portions by subtracting the 3D images of the preserved portions (after the sampling) from the images of the intact specimens (before the sampling) by using reverse engineering techniques; f) the prototyping of the missing/sampled portions to be integrated; g) the painting and application of the prototypes through the use of compatible and reversible adhesives.

* Corresponding author.
E-mail address: antonino.vazzana2@unibo.it (A. Vazzana).

https://doi.org/10.1016/j.jasrep.2022.103511
Received 15 February 2022; Received in revised form 16 May 2022; Accepted 3 June 2022

By following the proposed protocol, in addition to the fabrication of a physical element which is faithful to the original, it was possible to obtain a remarkable correspondence between the contact surfaces of the two portions (the original and the reconstructed one) without having to resort to any manipulation/adaptation of either element.

1. Introduction

In paleoanthropological research, dental and osteological remains are an irreplaceable source of information about the life history of an individual and the community to which this individual/person belonged. In recent years, the application of physicochemical (e.g., radiocarbon and uranium, stable isotope analysis, paleohistology, trace element analysis) and biomolecular analyses (e.g., ancient DNA, paleoproteomics) has revolutionized the field of osteoarchaeology and paleoanthropology. Even though they involve, in most cases, destructive or micro-destructive analyses, their application has become fundamental in the bioarchaeological field, allowing the retrieval of information that is not accessible through the employment of other non-destructive methodologies (e.g. Bortolini et al., 2021; Lugli et al., 2019; 2018; Nava et al., 2020; Slon et al., 2018; Sorrentino et al., 2018). Therefore, standard protocols are needed to plan integrative restoration before the samples are even collected and need to consider the state of preservation of the specimens (size and morphology, as well as physicochemical properties) and their possible use after restoration (e.g., further scientific research, exhibition, teaching).

Traditionally, the reconstruction requires a manual approach, which is strongly influenced by the experience and subjectivity of the operator, is highly invasive, and becomes more demanding the more severely damaged and morphologically complex is the region to be reconstructed. So far, the replacement of missing parts has involved the reproduction of the external integrity of the specimen either by applying dental wax or hot paste made of organic and inorganic components (modelling chalk, raw beeswax, resin, zinc white) or by using mold-based techniques for contact replication of the missing parts, as a means to facilitate future interpretations of the element (Cencetti, 2008; Colli et al., 2009; White et al., 2000; Zanolli et al., 2016).

In the past decades, high-resolution 2D and 3D imaging technologies have generated a considerable degree of interest for several applications. Examples of the fields of application are palaeoanthropology, archaeology, geology, civil engineering, archaeology, reverse engineering, medicine, and virtual reality (Higgins et al., 2020; Sansoni et al., 2009; Traversari et al., 2016; Vazzana et al., 2018). This has led to a remarkable development of virtual restoration methodologies with reverse engineering (RE) techniques (Cook et al., 2021; Haile-Selassie et al., 2019a; Senck et al., 2013), to the increasingly widespread use of rapid prototyping (RP) to create replicas and scale reproductions of movable and immovable objects (D'Urso et al., 2000; Pérès et al., 2004; Tucci and Bonora, 2012; Urcia et al., 2018) or, in rare cases, to the manufacture of missing parts that are useful for restoration (Fantini et al., 2008). A virtual anthropological approach (Benazzi et al., 2014a; 2011; Romandini et al., 2020; Senck et al., 2013; Weber, 2014; Weber and Bookstein, 2011; Zollikofer and Ponce de León, 2005) based on reverse engineering, computer-aided design (CAD) and rapid prototyping technologies can facilitate and improve these operations because they minimize the subjective choices of the operator and increase the reliability of the result.

At present, the virtual reconstruction and rapid prototyping of missing parts are mainly used in maxillofacial surgery, where the design of customized implants using CT-derived 3D models, combined with the development of new biocompatible materials and rapid prototyping technologies, has led to multiple advantages over traditional surgical techniques (Aimar et al., 2019; Chua et al., 2020; Giovacchini et al., 2021; Maglitto et al., 2021; Sandeep Kumar et al., 2018; Touri et al., 2019; Zhou et al., 2010). The ability to use and manipulate digital data from CT scans and form an exact replica of an osteo-archaeological object in different materials (resin, polylactic acid (PLA), acrilonitrile-butadiene-stirene (ABS), etc.) using RP technologies introduces a new dimension to modern osteology, restoration, and exhibition.

Here we provide clear guidelines for the reconstruction of dental elements (though also applicable to bones) from archaeological and palaeoanthropological contexts by combining traditional methods and tools developed in manufacturing industries, as well as in the field of medicine and other research fields. The present approach overcomes the limits of manual procedures by a) strongly reducing the handling of the specimen, ultimately reducing risks of damage; b) exploring alternative solutions for both digital and physical reconstructions; c) printing copies of the final product that can be used for, e.g., scientific purposes, exhibition, educational or promotional activities.

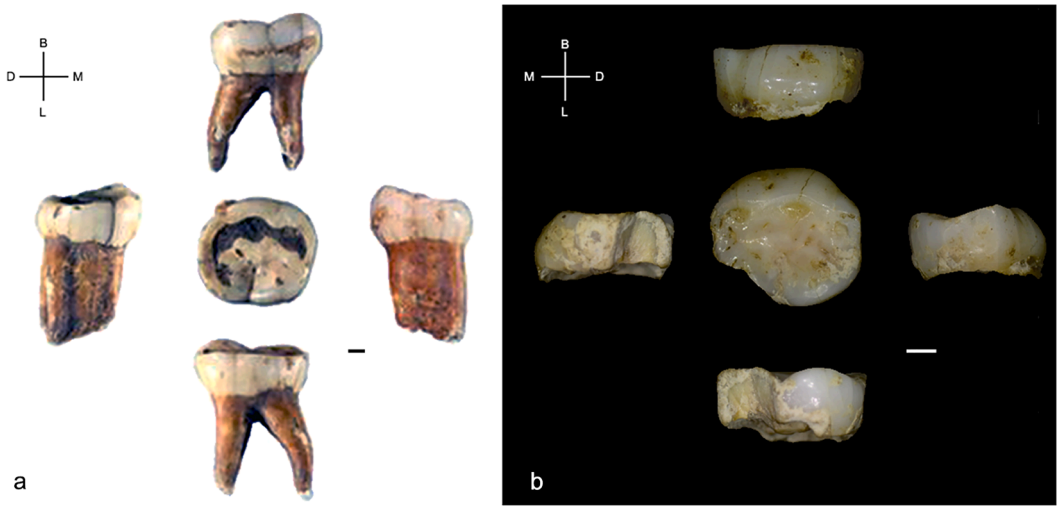

Fig. 1. Photographic record of the two findings before sampling. a) Roccia San Sebastiano 2 (RSS2), Ldm2; b) Pradis 1, Rdm2. Abbreviations: B = buccal; D = distal; L = lingual; M = mesial. Scale bar is 2 mm.

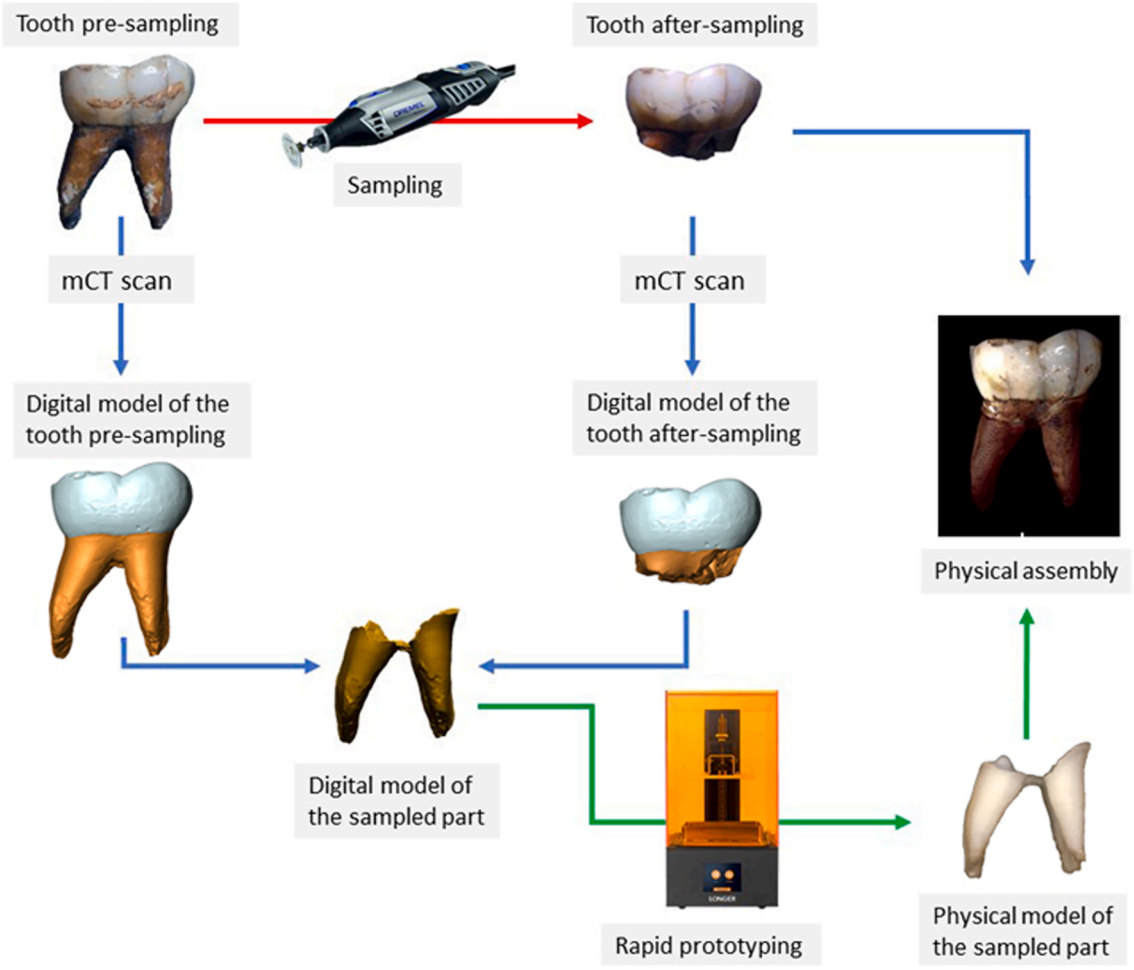

Fig. 2. Schematic of the different phases of integrative restoration protocol.

2. Materials

Our experiment of integrative restoration aimed at reconstructing the original morphology of dental finds was carried out on two human teeth from Upper Paleolithic contexts that were sampled for physico-chemical and molecular analyses.

Case. *Study* 1: *A human tooth from the archaeological excavation of Roccia San Sebastiano* (*Mondragone*, *Caserta*, *southern Italy*) (Collina et al., 2020). *The tooth* (*RSS2*) *is a worn* (*wear stage* 5 (Molnar, 1971)) *lower left second deciduous molar* (Ldm_2) *with a completed crown, a root preserved in its entirety and an open apical foramen* (Fig. 1*a*). *The development of the root suggests that the tooth was lost post-mortem, at an age ranging between* 4 (*age of eruption of the tooth*) *and* 6 *years* (*due to the absence of the distal interproximal contact facet*). *The find is stratigraphically associated with the Uluzzian* (Fig. 1*a*).

Case. *Study* 2: *A human tooth from level* 1*a of the archaeological excavation of Riparo I of Grotte Verdi di Pradis* (*Clauzetto*, *Pordenone*, *north-eastern Italy*) (Gurioli et al., 2011; Nannini et al., 2022). *The tooth* (*Pradis* 1, Fig. 1*b*) *is an exfoliated lower right second deciduous molar* (Rdm_2), *recovered from the Epigravettian layers of Grotte di Pradis*, *which was lost ante-mortem by an* 11-12-*year-old child. A direct radiocarbon date provided an age of* 13,088-12,897 *cal BP* (2σ, *IntCal*20) (Lugli et al, 2022).

3. Methods

The here-described protocol for physical restoration involved various stages: a) microCT of the original specimens; b) sampling; c) microCT of the specimens after sampling; d) reconstruction of the digital 3D surfaces of the specimens before and after sampling; e) creation of digital models of the missing/sampled portions by subtracting the 3D images of the preserved portions (after the sampling) from the images of the intact specimens (before the sampling) by using reverse engineering techniques; f) prototyping of the missing/sampled portions to be integrated; g) painting and application of the prototypes through the use of compatible and reversible adhesives (Fig. 2).

a) The teeth were measured using microcomputed tomography scanners (see Table 1, and SI).
b) The teeth were sampled with a diamond blade. RSS2 had its root separated from the crown to obtain 260 mg for aDNA (160 mg) and radiocarbon analyses (100 mg) (Fig. 3a); whereas Pradis 1 had its crown sectioned along the bucco-lingual plane (Fig. 3b) for histomorphometry (a ca. 800 μm section), strontium isotope (1 mg), radiocarbon dating (102 mg), proteomic sexing (<1 mg) and aDNA analyses (ca. 200 mg).The sectioning of Pradis 1 was performed at the Service of Bioarchaeology of the Museum of Civilizations, Rome. Dental tissues sampling of both specimens took place in the aDNA clean laboratory of the Department of Cultural Heritage of the University of Bologna, in Ravenna. The sample was cut inside a laminar flow hood, designed for ancient DNA sampling, allowing very low levels of background contamination.
c) An additional computed tomographic scan was performed on the teeth following the sampling (see Table 1, and Suppl. Inf.).
d) MicroCT image data (pre- and post-sampling) were segmented semi-automatically using Avizo Lite 9.2.0 software (Thermo Fisher

Table 1
Microcomputed tomography scanning parameters.

Specimen	Instrument location	Source	Voltage	Current	Filtration	Projections over 360°	Scan time	Data correction	Tomographic reconstruction algorithm	Voxel size of the reconstructed volume
RSS2	Department of Physics and Astronomy of the University of Bologna	sealed polychromatic microFocus X-ray tube (Thermo Kevex PXS10-65) and water-cooled VHR 4008x2672 CCD camera (Photonic Science).	130 kVp	1.32 mAs/ projection	0.1 mm Fe filtration	900	279 min	Beam hardening correction	Parallelized Feldkamp algorithm	Array of 950 × 950 × 770 cubic voxels, each with a side length of 13.8 μm
RSS2 after sampling	Department of Physics and Earth Science of the University of Ferrara	microfocus X-ray tube (Hamamatsu L9421)	70 kVp	0.1 mAs	0.5 mm Al	360	20 min	Beam hardening correction	FDK algorithm	Isotropic voxel size of 30 μm
Printed portion of RSS2	Department of Physics and Earth Science of the University of Ferrara	microfocus X-ray tube (Hamamatsu L9421)	50 kVp	0.1 mAs	0.5 mm Al	360	20 min	Beam hardening correction	FDK algorithm	Isotropic voxel size of 30 μm
Pradis 1	TomoLab laboratory at Elettra Sincrotrone Trieste	mirofocus X-ray tube (Hamamatsu L9181)	130 kVp	61 μA	1.5 mm Al	2400	280 min	Beam hardening correction, ring artefacts removal	FDK algorithm	Isotropic voxel size of 5.55 μm
Pradis 1 after sampling	Department of Physics and Earth Science of the University of Ferrara	microfocus X-ray tube (Hamamatsu L9421)	70 kVp	0.1 mAs	0.5 mm Al	360	20 min	Beam hardening correction	FDK algorithm	Isotropic voxel size of 30 μm
Printed portion of Pradis 1	Department of Physics and Earth Science of the University of Ferrara	microfocus X-ray tube (Hamamatsu L9421)	50 kVp	0.1 mAs	0.5 mm Al	360	20 min	Beam hardening correction	FDK algorithm	Isotropic voxel size of 30 μm

Scientific) to render the pre- and post-sampling 3D digital models (Galibourg et al., 2018; Naumovich et al., 2015), which were then imported in Geomagic Design X (3D Systems) for cleaning processes and for the correction of incidental defects (e.g., filling of small holes) to create fully closed surfaces (Fig. 4).

e) Case Study 1: Following procedures described in Benazzi et al., (2014b), three different spline curves were digitized on the margins of the artificial cut (one on the external margin and two on the margin of the root canals) of the post-sampling digital model to isolate the cutting surface and create a negative version of it. The pre- and post-sampling digital models were overlaid using the superimposition algorithm on Geomagic Design X software, and the previously created spline curves were projected onto the digital model of the whole tooth (pre-sampling) to isolate the sampled portion (Fig. 5a). Then, the negative of the cutting surface and the model of the sampled portion were merged in a single mesh and any discontinuity was removed (Cook et al., 2021; Haile-Selassie et al., 2019b) (Fig. 5a).

Case. *Study* 2: *The digital surfaces* (*of the dental crown pre- and post-sampling*) *were superimposed using the superimposition algorithms present in Geomagic Design X software. In order to extract the missing portion of the tooth, a best fit plane was generated on the surface of the sampling cut present on the model of the preserved fragment* (*post-sampling*). *This same plane was then used to divide the digital model of the whole tooth into two portions*: *the sampled one and the preserved one. After that, the surface of the cut was isolated and its negative stitched to the sampled portion* (Fig. 5*b*). *This resulted in a distinct three-dimensional model complementing what is left of the original* (Fig. 5*b*).

f) Exact replicas of the sampled portions were reproduced with rapid prototyping technology (LCD Stereolithography (SLA)) using an Orange 10 LCD 3D printer (Longer). The prototype was produced using Longer UV resin with a layer thickness of 0.05 mm, UV Matrix 405 nm LED lighting sources and slicing Longerware software (Longer).

g) Finally, the printed replicas of the root of case study 1 and of half of the dental crown of case study 2 were painted and applied onto the preserved original portions by using compatible and reversible glues (specifically UHU extra gel Polyvinylester) (Figs. 6 and 7).

To determine the accuracy of the replicas, the standard deviation between the surfaces of the original specimens and the ones of the prototyped products was calculated. To do this, the printed portions were also acquired through computerized micro-tomography (see Table 1, and Suppl. Inf.), and their digital 3D surfaces (generated by following the segmentation methodologies described previously) were compared with the ones generated from the microCTs of the specimens prior to sampling by applying the standard deviation tool in Geomagic Design X between the meshes (Benazzi, 2008).

4. Results

The mesh/mesh deviation plot illustrates the average absolute deviation between the superimposed digital models of the virtual integration and of the resin prototypes for both case studies (Figs. 8 and 9). The standard deviation (SD) recorded for the root of RSS2 is 0.2 mm, with a mean deviation of 0.06 mm when considering the entire model. The measured deviation values for the contact surface range from 0.1 mm to −0.1 mm. On the other hand, for the crown of Pradis1, the SD is 0.3 mm, with a mean deviation of 0.07 mm, whereas the deviation values recorded for the contact surface are between 0 mm and −0.2 mm. The increase – although still very low – of deviation values when looking at the contact surfaces can be explained by the constrictions set by the

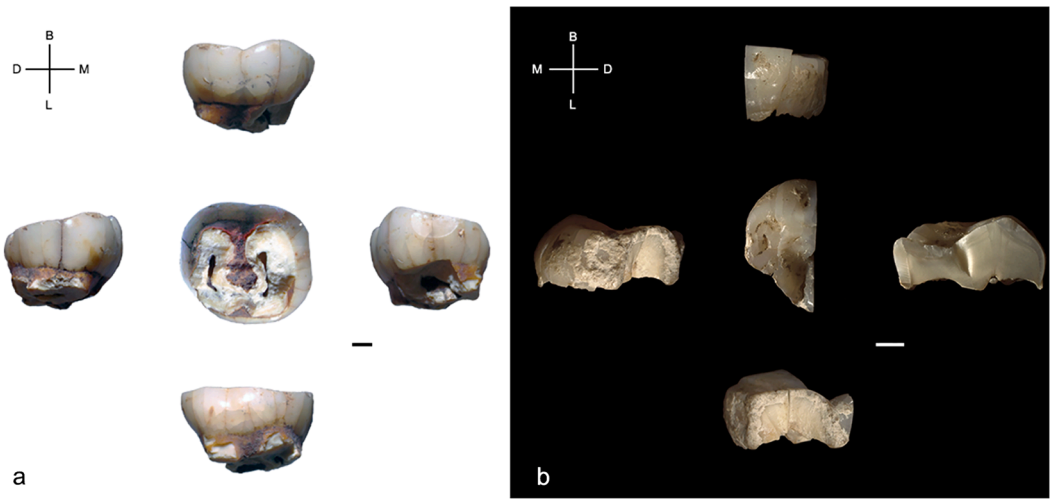

Fig. 3. Photographic record of the two findings after sampling. a) Roccia San Sebastiano 2 (RSS2), Ldm_2, periapical view in the center; b) Pradis 1, Rdm_2. Abbreviations: B = buccal; D = distal; L = lingual; M = mesial. Scale bar is 2 mm.

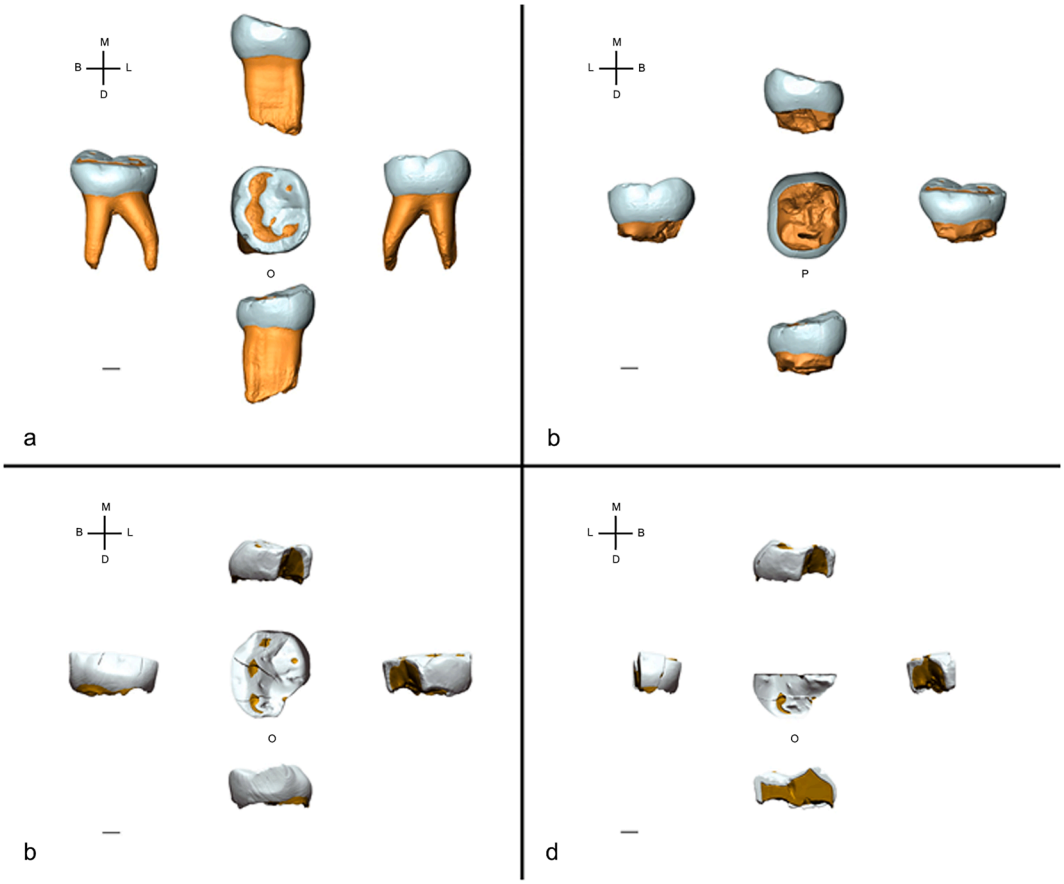

Fig. 4. Digital models of RSS2 and Pradis 1 before (a, c) and after (b, d) sampling, in all views. Abbreviations: B = buccal; D = distal; L = lingual; M = mesial; O = occlusal; P = periapical. Scale bar is 2 mm.

3D printer and the minimum allowed thickness of the printed layer. The minimal differences recorded between the contact surfaces allowed the application of the prototypes to the original specimens without having to make any kind of adjustment (Figs. 6 and 7).

5. Conclusions

The outline of protocols designed for the accurate reconstruction of the morphological integrity of dental specimens and, in general, of osteological finds after sampling for chemical, physical and molecular analyses is becoming more and more of a necessity. The information that can be obtained through the application of this type of analyses, which are usually destructive or micro-destructive, has become essential to reconstruct with greater detail the life history of an individual.

The main intent of this work is to introduce a standardized methodology that can be used to restore the original morphology of biological

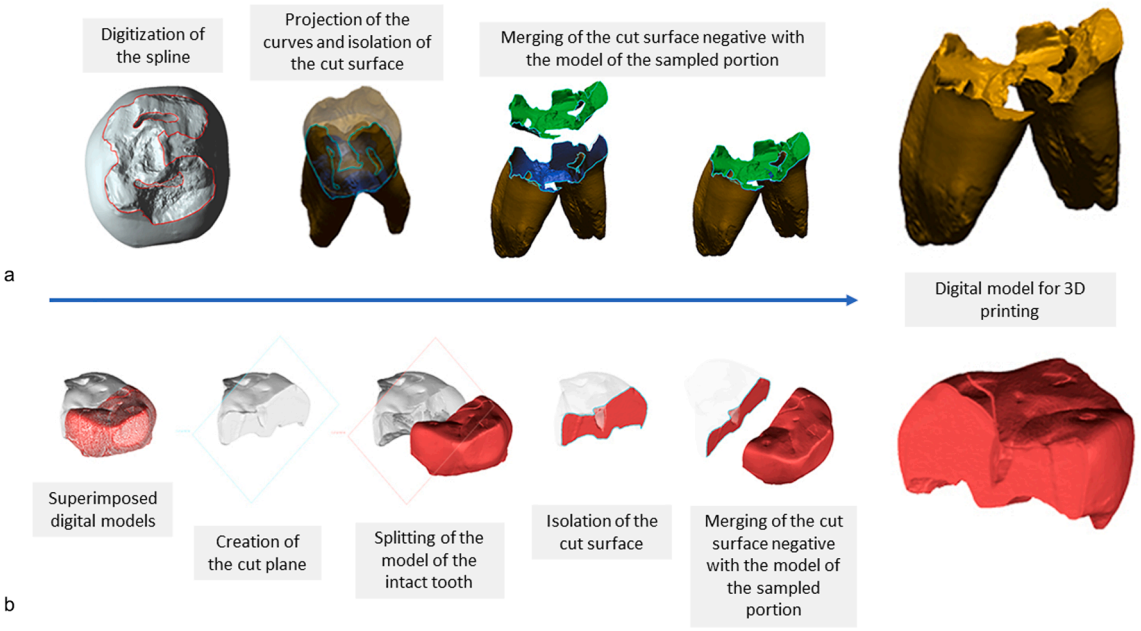

Fig. 5. Schematic of the protocol for the creation of digital models of missing/sampled portion by using reverse engineering techniques. a) case study 1: Roccia San Sebastiano 2 (RSS2), Ldm_2; b) case study 2: Pradis 1, Rdm_2.

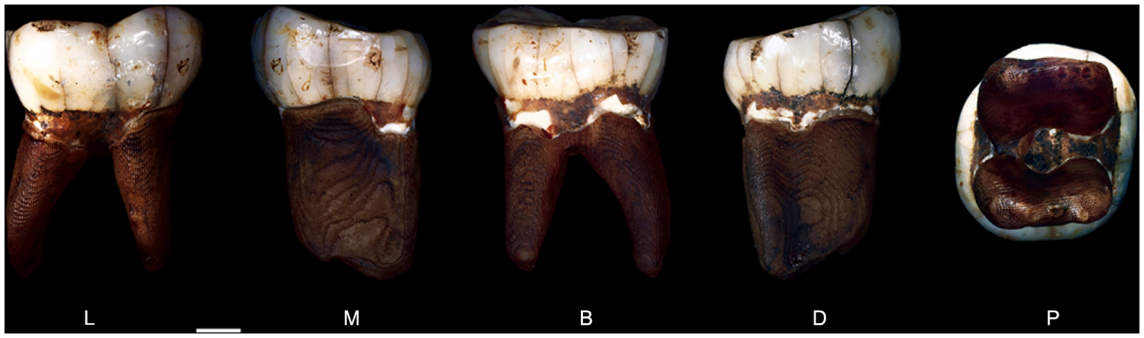

Fig. 6. Photographic record of RSS2 (Ldm_2) after physical restoration; L = lingual; M = mesial; B = buccal; D = distal; P = periapical. Scale bar is 2 mm.

Fig. 7. Photographic record of Pradis 1 (Rdm_2) tooth after physical restoration; O = occlusal; B = buccal; M = mesial; P = periapical; L = lingual; D = distal. Scale bar is 2 mm.

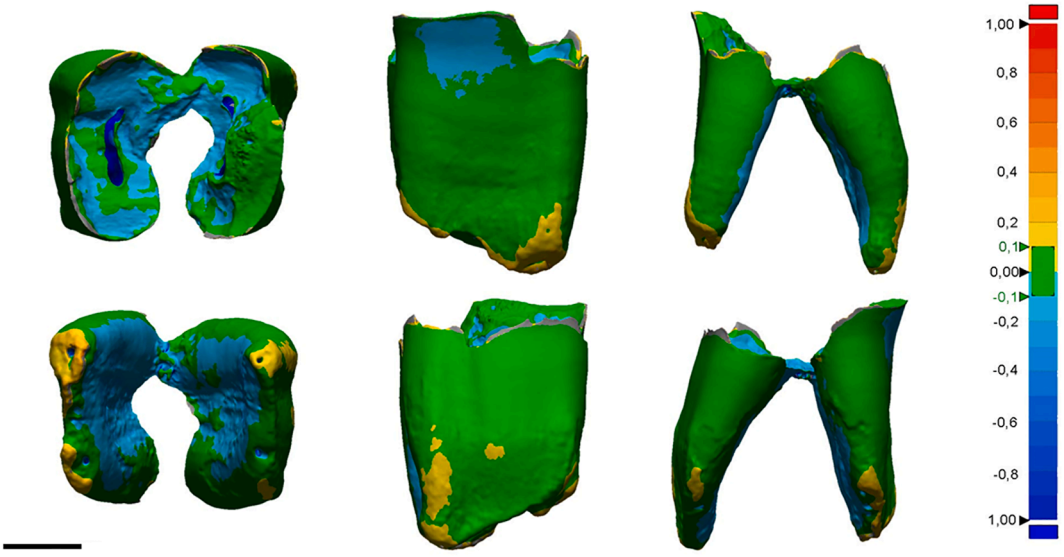

Fig. 8. RSS2, standard deviation plot of the digital surfaces of the original portion and the 3D printed integrative portion. Scale bar is 2 mm.

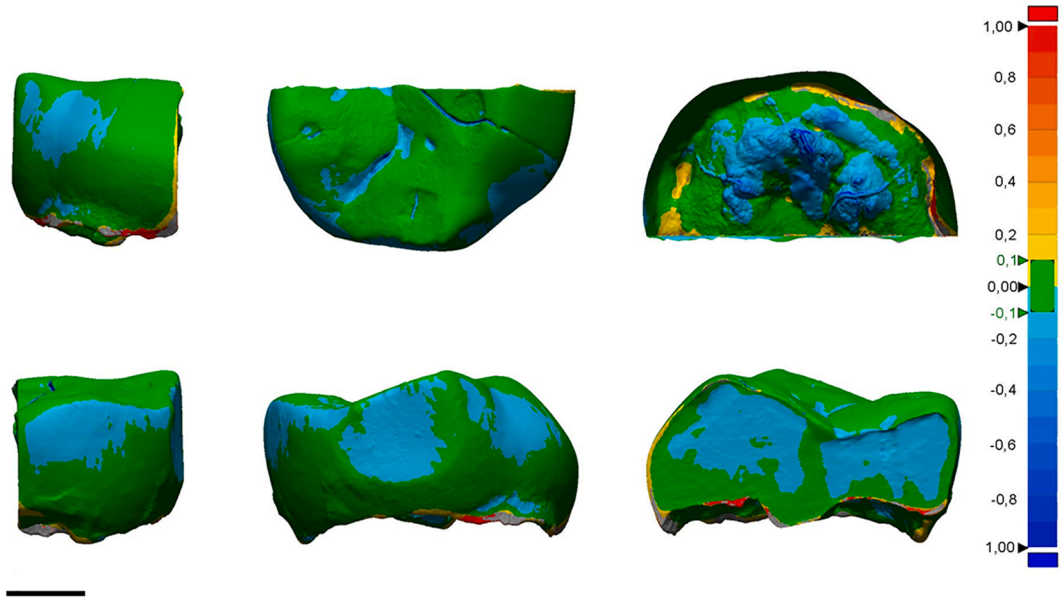

Fig. 9. Pradis 1, standard deviation plot of the digital surfaces of the original portion and the 3D printed integrative portion. Scale bar is 2 mm.

findings (teeth, but also bones) sampled for chemical, physical and molecular analyses by using rapid prototyping techniques. The case studies here presented testify that the integration between RE, CAD and RP can help develop innovative restoration protocols characterized by a non-invasive and reversible approach. This method allows a more thorough planning of any invasive sampling intervention, opening new perspectives in the bioarchaeological field.

The mold-based techniques that are currently in use for physical restoration are well-tested, but much more rudimentary. They produce good results but cannot be used without physical manipulation of the original object, which serves as a model. This increases the risk of damaging or altering the find, whereas digital technology allows to overcome this problem. The proposed method allows the design of the prototype of the missing/sampled portion through microCT analysis and 3D printing, and its application onto the preserved portion with minimal manipulation of the object. The accuracy and reproducibility of the models provide a more durable, yet still tangible subject to study. In addition, in the case of museum exhibits, the viewer is enabled to appreciate the entire shape of the object, which – if necessary – can also be scaled, increasing cognitive perception.

Currently, possible limitations of this methodology are related to RP materials, as there are no studies about their compatibility, strength, durability, and aging in different storage environments. Moreover, the time and resource investment (as well as the access to specific equipment) this method involves implies it should not be required as a general standard restoration protocol, but rather a high accuracy method to be applied on the most significant specimens.

Our protocol, like the ones regarding virtual restoration with geometric morphometry techniques (Cook et al., 2021; Haile-Selassie et al., 2019a; Talamo et al., 2021), has the potential to revolutionize the field of restoration, not only of osteological finds, but also of movable and immovable objects of historical, artistic and archaeological interest like sculptures, bas-reliefs, architectural elements, and ceramics. In addition, its application can also impact the medical/orthopaedic field and

improve the protocols that are currently in use in the creation of implants, which often need to be completely finished before implantation.

Declaration of Competing Interest

The authors declare that they have no known competing financial interests or personal relationships that could have appeared to influence the work reported in this paper.

Acknowledgments

The authors thank the Friuli Venezia Giulia and Salerno, Avellino, Benevento, Caserta Superintendencies for providing access to the skeletal materials. This project was funded by the European Research Council (ERC) under the European Union's Horizon 2020 Research and Innovation Programme (Grant Agreement no. 724046–SUCCESS awarded to S.B.).

Appendix A. Supplementary data

Supplementary data to this article can be found online at https://doi.org/10.1016/j.jasrep.2022.103511.

References

Aimar, A., Palermo, A., Innocenti, B., 2019. The role of 3D printing in medical applications: a state of the art. J. Healthcare Eng. 2019, 1–10.

Benazzi, S., 2008. Evaluating humeral bilateral asymmetry by means of a virtual 3D approach Evaluating Humeral Bilateral Asymmetry by Means 1–8.

Benazzi, S., Bookstein, F.L., Strait, D.S., Weber, G.W., 2011. A new OH5 reconstruction with an assessment of its uncertainty. J. Hum. Evol. 61, 75–88. https://doi.org/10.1016/j.jhevol.2011.02.005.

Benazzi, S., Gruppioni, G., Strait, D.S., Hublin, J.-J., 2014a. Technical Note: virtual reconstruction of KNM-ER 1813 *Homo habilis* cranium. Am. J. Phys. Anthropol. 153, 154–160. https://doi.org/10.1002/ajpa.22376.

Benazzi, S., Panetta, D., Fornai, C., Toussaint, M., Gruppioni, G., Hublin, J.-J., 2014b. Technical Note: Guidelines for the digital computation of 2D and 3D enamel thickness in hominoid teeth. Am. J. Phys. Anthropol. 153, 305–313. https://doi.org/10.1002/ajpa.22421.

Bortolini, E., Pagani, L., Oxilia, G., Posth, C., Fontana, F., Badino, F., Saupe, T., Montinaro, F., Margaritora, D., Romandini, M., Lugli, F., Papini, A., Boggioni, M., Perrini, N., Oxilia, A., Cigliano, R.A., Barcelona, R., Visentin, D., Fasser, N., Arrighi, S., Figus, C., Marciani, G., Silvestrini, S., Bernardini, F., Menghi Sartorio, J. C., Fiorenza, L., Cecchi, J.M., Tuniz, C., Kivisild, T., Gianfrancesco, F., Peresani, M., Scheib, C.L., Talamo, S., D'Esposito, M., Benazzi, S., 2021. Early Alpine occupation backdates westward human migration in Late Glacial Europe. Curr. Biol. 31 (11), 2484–2493.e7.

Cencetti, S., 2008. Strumenti, materiali e tecniche finalizzati alla conservazione e alla valorizzazione di vertebrati fossili. Museol. Sci. Mem. 3, 61–68.

Chua, C.K., Leong, K.F., An, J., 2020. Introduction to rapid prototyping of biomaterials, in: Rapid Prototyping of Biomaterials. Elsevier, pp. 1–15. https://doi.org/10.1016/B978-0-08-102663-2.00001-0.

Colli, L., Cencetti, S., Salvini, A., Pecchioni, E., 2009. Collezioni paleontologiche storiche: materiali di restauro e problematiche di conservazione. Museol. Sci. 3 (1–2), 76–82.

Collina, C., Marciani, G., Martini, I., Donadio, C., Repola, L., Bortolini, E., Arrighi, S., Badino, F., Figus, C., Lugli, F., Oxilia, G., Romandini, M., Silvestrini, S., Piperno, M., Benazzi, S., 2020. Refining the Uluzzian through a new lithic assemblage from Roccia San Sebastiano (Mondragone, southern Italy). Quat. Int. 551, 150–168. https://doi.org/10.1016/j.quaint.2020.03.056.

Cook, R.W., Vazzana, A., Sorrentino, R., Benazzi, S., Smith, A.L., Strait, D.S., Ledogar, J. A., 2021. The cranial biomechanics and feeding performance of Homo floresiensis. Interface Focus 11 (5), 20200083.

D'Urso, P.S., Thompson, R.G., Earwaker, W.J., 2000. Stereolithographic (SL) biomodelling in palaeontology: a technical note. Rapid Prototyp. J. 6, 212–215. https://doi.org/10.1108/13552540010372471.

Fantini, M., De Crescenzio, F., Persiani, F., Benazzi, S., Gruppioni, G., 2008. 3D restitution, restoration and prototyping of a medieval damaged skull. Rapid Prototyp. J. 14, 318–324. https://doi.org/10.1108/13552540810907992.

Galibourg, A., Dumoncel, J., Telmon, N., Calvet, A., Michetti, J., Maret, D., 2018. Assessment of automatic segmentation of teeth using a watershed-based method. Dentomaxillofacial Radiol. 47, 47. https://doi.org/10.1259/DMFR.20170220.

Giovacchini, F., Gilli, M., Mitro, V., Monarchi, G., Bensi, C., Tullio, A., 2021. Rapid prototyping: applications in oral and maxillofacial surgery. J. Oral Med. Oral Surg. 27, 11. https://doi.org/10.1051/mbcb/2020050.

Gurioli, F., Bartolomei, G., Nannini, N., Peresani, M., Romandini, M., 2011. Deux clavicules de marmotte épigravettiennes incisées provenant des grottes Verdi de Pradis (Alpes italiennes)Two Epigravettian engraved marmot clavicles from the Grottes Verdi de Pradis (Alpes italiennes). PALEO. Rev. d'archéologie préhistorique (22), 311–318.

Haile-Selassie, Y., Melillo, S.M., Vazzana, A., Benazzi, S., Ryan, T.M., 2019a. A 3.8-million-year-old hominin cranium from Woranso-Mille, Ethiopia. Nature 573 (7773), 214–219.

Haile-Selassie, Y., Melillo, S.M., Vazzana, A., Benazzi, S., Ryan, T.M., 2019b. A 3.8-million-year-old hominin cranium from Woranso-Mille, Ethiopia. Nature 573, 214–219. https://doi.org/10.1038/s41586-019-1513-8.

Higgins, O.A., Vazzana, A., Scalise, L.M., Riso, F.M., Buti, L., Conti, S., Bortolini, E., Oxilia, G., Benazzi, S., 2020. Comparing traditional and virtual approaches in the micro-excavation and analysis of cremated remains. J. Archaeol. Sci. Reports 32, 102396. https://doi.org/10.1016/j.jasrep.2020.102396.

Lugli, F., Cipriani, A., Tavaglione, V., Traversari, M., Benazzi, S., 2018. Transhumance pastoralism of Roccapelago (Modena, Italy) early-modern individuals: Inferences from Sr isotopes of hair strands. Am. J. Phys. Anthropol. 167, 470–483. https://doi.org/10.1002/ajpa.23643.

Lugli, F., Di Rocco, G., Vazzana, A., Genovese, F., Pinetti, D., Cilli, E., Carile, M.C., Silvestrini, S., Gabanini, G., Arrighi, S., Buti, L., Bortolini, E., Cipriani, A., Figus, C., Marciani, G., Oxilia, G., Romandini, M., Sorrentino, R., Sola, M., Benazzi, S., 2019. Enamel peptides reveal the sex of the Late Antique 'Lovers of Modena'. Sci. Rep. 9 https://doi.org/10.1038/s41598-019-49562-7.

Lugli, F., Nava, A., Sorrentino, R., Vazzana, A., Bortolini, E., Oxilia, G., Sara, S., Nannini, N., Bondioli, L., Fewlass, H., Talamo, S., Bard, E., Mancini, L., Müller, W., Romandini, M., Benazzi, S., 2022. Tracing the mobility of a Late Epigravettian (~13 ka) male infant from Grotte di Pradis (Northeastern Italian Prealps) at high-temporal resolution. Sci. Rep. 41598 https://doi.org/10.1038/s41598-022-12193-6.

Maglitto, F., Dell, G., Orabona, A., Committeri, U., Salzano, G., Renato De Fazio, G., Angelo Vaira, L., Abbate, V., Bonavolontà, P., Piombino, P., Califano, L., 2021. Virtual surgical planning and the "in-house" rapid prototyping technique in maxillofacial surgery: the current situation and future perspectives. https://doi.org/10.3390/app11031009.

Molnar, S., 1971. Human tooth wear, tooth function and cultural variability. Am. J. Phys. Anthropol. 34 (2), 175–189. https://doi.org/10.1002/ajpa.1330340204.

Nannini, N., Duches, R., Fontana, A., Romandini, M., Boschin, F., Crezzini, J., Peresani, M., 2022. Marmot hunting during the Upper Palaeolithic: The specialized exploitation at Grotte di Pradis (Italian pre-Alps). Quat. Sci. Rev. 277, 107364 https://doi.org/10.1016/j.quascirev.2021.107364.

Naumovich, S.S., Naumovich, S.A., Goncharenko, V.G., 2015. Three-dimensional reconstruction of teeth and jaws based on segmentation of CT images using watershed transformation. Dentomaxillofac. Radiol. 44 (4), 20140313.

Nava, A., Lugli, F., Romandini, M., Badino, F., Evans, D., Helbling, A.H., Oxilia, G., Arrighi, S., Bortolini, E., Delpiano, D., Duches, R., Figus, C., Livraghi, A., Marciani, G., Silvestrini, S., Cipriani, A., Giovanardi, T., Pini, R., Tuniz, C., Bernardini, F., Dori, I., Coppa, A., Cristiani, E., Dean, C., Bondioli, L., Peresani, M., Müller, W., Benazzi, S., 2020. Early life of Neanderthals. Proc. Natl. Acad. Sci. USA 117, 28719–28726. https://doi.org/10.1073/pnas.2011765117.

Pérès, F., Taha, F., De Lumley, M.A., Cabanis, E., 2004. Digital modelling and stereolithographic production of a Homo Erectus skull. Rapid Prototyp. J. 10, 247–254. https://doi.org/10.1108/13552540410551379.

Romandini, M., Oxilia, G., Bortolini, E., Peyrégne, S., Delpiano, D., Nava, A., Panetta, D., Di Domenico, G., Martini, P., Arrighi, S., Badino, F., Figus, C., Lugli, F., Marciani, G., Silvestrini, S., Menghi Sartorio, J.C., Terlato, G., Hublin, J.-J., Meyer, M., Bondioli, L., Higham, T., Slon, V., Peresani, M., Benazzi, S., 2020. A late Neanderthal tooth from northeastern Italy. J. Hum. Evol. 147, 102867 https://doi.org/10.1016/j.jhevol.2020.102867.

Sandeep Kumar, Y., Rao Kvs, R., Yalamalle, S.R., Venugopal, S.M., Krishna, S., 2018. Applications of 3D printing in TKR Pre surgical planning for Design Optimization - A Case Study, in: Materials Today: Proceedings. Elsevier Ltd, pp. 18833–18838. https://doi.org/10.1016/j.matpr.2018.06.230.

Sansoni, G., Trebeschi, M., Docchio, F., 2009. State-of-the-art and applications of 3D imaging sensors in industry, cultural heritage, medicine, and criminal investigation. Sensors 9, 568–601. https://doi.org/10.3390/s90100568.

Senck, S., Coquerelle, M., Weber, G.W., Benazzi, S., 2013. Virtual reconstruction of very large skull defects featuring partly and completely missing midsagittal planes. Anat. Rec. 296, 745–758. https://doi.org/10.1002/ar.22693.

Slon, V., Mafessoni, F., Vernot, B., de Filippo, C., Grote, S., Viola, B., Hajdinjak, M., Peyrégne, S., Nagel, S., Brown, S., Douka, K., Higham, T., Kozlikin, M.B., Shunkov, M.V., Derevianko, A.P., Kelso, J., Meyer, M., Prüfer, K., Pääbo, S., 2018. The genome of the offspring of a Neanderthal mother and a Denisovan father. Nature 561, 113–116. https://doi.org/10.1038/s41586-018-0455-x.

Sorrentino, R., Bortolini, E., Lugli, F., Mancuso, G., Buti, L., Oxilia, G., Vazzana, A., Figus, C., Serrangeli, M.C., Margherita, C., Penzo, A., Gruppioni, G., Gottarelli, A., Jochum, K.P., Belcastro, M.G., Cipriani, A., Feeney, R.N.M., Benazzi, S., Caramelli, D., 2018. Unravelling biocultural population structure in 4th/3rd century BC Monterenzio Vecchio (Bologna, Italy) through a comparative analysis of strontium isotopes, non-metric dental evidence, and funerary practices. PLoS One 13 (3), e0193796.

Talamo, S., Urbanowski, M., Picin, A., Nowaczewska, W., Vazzana, A., Binkowski, M., Cercatillo, S., Diakowski, M., Fewlass, H., Marciszak, A., Paleček, D., Richards, M.P., Ryder, C.M., Sinet-Mathiot, V., Smith, G.M., Socha, P., Sponheimer, M., Stefaniak, K., Welker, F., Winter, H., Wiśniewski, A., Żarski, M., Benazzi, S., Nadachowski, A., Hublin, J.J., 2021. A 41,500 year-old decorated ivory pendant from Stajnia Cave (Poland). Sci. Rep. 11, 1–11. https://doi.org/10.1038/s41598-021-01221-6.

Touri, M., Kabirian, F., Saadati, M., Ramakrishna, S., Mozafari, M., 2019. Additive manufacturing of biomaterials – The evolution of rapid prototyping. Adv. Eng. Mater. 21, 1800511. https://doi.org/10.1002/adem.201800511.

Traversari, M., Feletti, F., Vazzana, A., Gruppioni, G., Frelat, M.A., 2016. Three cases of developmental dysplasia of the hip on partially mummified human remains (Roccapelago, Modena, 18th Century): a study of palaeopathological indicators through direct analysis and 3D virtual models. Bull. Mem. Soc. Anthropol. Paris 28 (3-4), 202–212.

Tucci, G., Bonora, V., 2012. From Real to... "Real". A review of geomatic and rapid prototyping techniques for solid modelling in cultural heritage field. ISPRS – Int. Arch. Photogramm. Remote Sens. Spat. Inf. Sci. XXXVIII-5/ 575–582. https://doi.org/10.5194/isprsarchives-xxxviii-5-w16-575-2011.

Urcia, A., Zambruno, S., Vazzana, A., Anderson, M., Darnell, C.M., 2018. Echoes of Egypt: Conjuring the Land of Pharaohs, 317–332.

Vazzana, A., Scalise, L.M., Traversari, M., Figus, C., Apicella, S.A., Buti, L., Oxilia, G., Sorrentino, R., Pellegrini, S., Matteucci, C., Calcagnile, L., Savigni, R., Feeney, R.N. M., Gruppioni, G., Benazzi, S., 2018. A multianalytic investigation of weapon-related injuries in a Late Antiquity necropolis, Mutina, Italy. J. Archaeol. Sci. Reports 17, 550–559.

Weber, G.W., 2014. Another link between archaeology and anthropology: Virtual anthropology. Digit. Appl. Archaeol. Cult. Herit. 1 (1), 3–11.

Weber, G.W., Bookstein, F.L. (Eds.), 2011. Virtual Anthropology. Springer Vienna, Vienna.

White, T.D., Folkens, P.A., Diego, S., Francisco, S., York, N., London, B., Tokyo, S., 2000. Human Osteology SECOND EDITION. Academic Press.

Zanolli, C., Dean, C., Rook, L., Bondioli, L., Mazurier, A., Macchiarelli, R., 2016. Enamel thickness and enamel growth in Oreopithecus: combining microtomographic and histological evidence. Comptes Rendus Palevol 15, 209–226. https://doi.org/10.1016/J.CRPV.2015.02.001.

Zhou, L.B., Shang, H.T., He, L.S., Bo, B., Liu, G.C., Liu, Y.P., Zhao, J.L., 2010. Accurate reconstruction of discontinuous mandible using a reverse engineering/computer-aided design/rapid prototyping technique: a preliminary clinical study. J. Oral Maxillofac. Surg. 68, 2115–2121. https://doi.org/10.1016/j.joms.2009.09.033.

Zollikofer, C.P.E., Ponce de León, M.S., 2005. Virtual reconstruction: a primer in computer-assisted paleontology and biomedicine. Wiley-Interscience.